Organic & Biomolecular Chemistry

ROYAL SOCIETY OF CHEMISTRY

PAPER

View Article Online
View Journal | View Issue

Cite this: *Org. Biomol. Chem.*, 2025, **23**, 7801

Ascidiolides, nitrogenous phthalides from the solitary ascidian *Ascidia virginea* from the Northeastern Atlantic, and structural revision of the closely related ascidines

Laurence K. Jennings,[a] Navdeep Kaur,[a] Maria C. Ramos,[b] Mercedes de la Cruz,[b] Maggie M. Reddy,[a] Fernando Reyes[b] and Olivier P. Thomas *[a]

As part of our investigation into the chemical diversity of Irish marine invertebrates, we identified the solitary ascidian *Ascidia virginea* as a promising organism. A fractionated extract from this organism exhibited toxicity in a brine shrimp assay and its chemical profiling indicated the presence of an unknown family of highly unsaturated nitrogenous metabolites. The targeted isolation and NMR based structural elucidation of members of this family led to the identification of four new phthalide derivatives, named ascidiolides A–D (**1–4**). The presence of a furanone ring was indicative of their similarity with both previously described polyaromatic butenolides from other ascidian species and isoquinolinediones isolated from the same species. Sixteen additional derivatives were characterised using only LC-MS/MS, HSQC NMR analysis, and analogy with major metabolites due to the minute amounts present in the extract. The unique structures of the ascidiolides allowed us to propose a biosynthetic pathway from anthranilic acid. Their structures also led to the revision of the structures of the ascidines A–C, related metabolites previously isolated from *A. virginea* collected in Norway. The isolated compounds **1–4** exhibited no cytotoxicity against a panel of tumour cell lines nor antimicrobial activity against several human pathogens, while the antioxidant activity measured for ascidiolide D (**4**) was comparable to that of the ascorbic acid positive control.

Received 25th July 2025,
Accepted 8th August 2025

DOI: 10.1039/d5ob01206f

rsc.li/obc

Introduction

Over the past half a century, ascidians, also referred to as sea squirts (Class Ascidiacea), have been found to produce a diverse and unique range of natural products with interesting bioactivities.[1] Importantly, two colonial ascidian natural products have been developed into medically approved treatments for cancer, trabectedin from *Ecteinascidia turbinata* and plitidepsin from *Aplidium albicans*.[2] An interesting class of metabolites produced by ascidians is the polyaromatic furanones. A considerable number of derivatives have previously been identified including the rubrolides, cadiolides, prunolides and procerolides.[3–6] These compounds often exhibit potent bioactivities and are considered interesting scaffolds for drug development. They are characterised by a central branched furanone ring formed by the condensation of two tyrosine derived hydroxyphenylpyruvic acid units, with at least one unit halogenated. With the proliferation of some solitary ascidian species in shallow marine waters, this chemical diversity is becoming readily available and could serve as scaffolds for drug development due to the large amount of biomaterial sometimes available.[7]

As part of our ongoing Marine Biodiscovery programme on Irish marine invertebrates,[8] the methanol fractions derived from an organic extract prepared from the common species *Ascidia virginea* exhibited activity in an *Artemia* lethality assay. Additionally, LC-MS screening indicated the presence of a large number of unknown nitrogenous and halogenated metabolites with a high degree of unsaturation.[9] This indicated similarity with the ascidines, a small group of halogenated nitrogenous metabolites previously reported from a specimen of *A. virginea* collected in Norway. These metabolites featured a unique isoquinolinedione unit not previously identified in other organisms.[10] However, using LC-MS we could not annotate any of the reported ascidines in our specimen collected from Ireland. Herein, we describe the isolation

[a]*School of Biological and Chemical Sciences, Ryan Institute, University of Galway, University Road, Galway H91 TK33, Ireland.*
E-mail: olivier.thomas@universityofgalway.ie
[b]*Fundación MEDINA, Centro de Excelencia en Investigación de Medicamentos Innovadores en Andalucía, Avda. del Conocimiento 34, Edificio Centro de Desarrollo Farmacéutico y Alimentario, Parque Tecnológico de Ciencias de la Salud, 18016 Granada, Spain*

and structural elucidation of four new phthalide metabolites from the Irish specimen of *A. virginea*. Following classical natural product isolation, a mixed analysis with MS/MS and NMR of the derived fractions enabled the characterisation of minor analogues.

Results and discussion

The freeze-dried biomass of *A. virginea* (3.8 g) was exhaustively extracted with a mixture of MeOH/CH_2Cl_2 (1 : 1 v : v). The resulting extract was then fractionated on C_{18}-silica gel with a stepwise gradient from H_2O to MeOH to CH_2Cl_2. The fraction that eluted with a 1 : 3 mixture of H_2O/MeOH was subjected to successive reverse phase HPLC purification yielding four new nitrogenated phthalide natural products named ascidiolide A–D (**1–4**) (Fig. 1).

Ascidiolide A (**1**) was isolated as a pale red amorphous solid and exhibited a protonated adduct $[M + H]^+$ in the (+) HRESIMS at *m*/*z* 258.0765, consistent with the molecular formula $C_{14}H_{11}NO_4$. This mass indicated that there were 10 degrees of unsaturation to be accounted for within the molecule. The ^{1}H NMR data contained resonances associated with six aromatic protons at δ_H 7.07 (d, J = 8.5 Hz, 2H), 6.92 (d, J = 7.6 Hz), 6.77 (d, J = 8.5 Hz, 2H) and 6.30 (dd, J = 7.6, 0.9 Hz), and one deshielded oxygenated methine at δ_H 6.25 (br s). The ^{13}C NMR data exhibited 12 resonances associated with one carbonyl (δ_C 174.2), six non-protonated aromatic carbons (δ_C 159.4, 145.0, 142.4, 138.0, 129.9 and 109.4), six aromatic methine carbons (δ_C 130.0, 121.0, 116.5 and 110.4) and one oxygenated methine carbon (δ_C 84.4). The symmetry of the two doublets at δ_H 7.07 (H-9/13) and 6.77 (H-10/12) and their HMBC correlations to δ_C 159.4 (C-11) and δ_C 129.9 (C-8), respectively, indicated the presence of a 4-hydroxyphenyl moiety. Another HMBC correlation from H-9/13 to δ_C 84.4 (C-3) indicated the linkage of this moiety to the oxygenated methine. The two aromatic doublets at δ_H 6.92 (H-5) and 6.30 (H-4) and their HMBC correlations to four other non-protonated aromatic carbons indicated the presence of a 1,2,3,4-tetrasubstituted aromatic ring. The H-4/C-3 and H-3/C-3a and C-4 HMBC correlations in conjunction with a small 0.9 Hz $^4J_{HH}$ coupling between H-4 and H-3 also established the direct link of the new tetrasubstituted ring to the oxygenated methine. A final HMBC correlation from H-3 to the δ_C 174.2 (C-1) carbonyl indicated that C-3 was connected to an ester oxygen. Based on the molecular formula determined, only an amine, a hydroxy group and a final degree of unsaturation were left to be assigned, suggesting that the three remaining substituents on the 1,2,3,4-tetrasubstituted aromatic ring were the C-1 carbonyl, a hydroxy group and an amine. Large $^3J_{CH}$ HMBC correlations were observed from H-4 to δ_C 145.0 (C-6) and 109.4 (C-7a), as well as from H-5 to C-3a and δ_C 138.0 (C-7), establishing the resonances in *meta* positions to each proton. The significant shielding of the C-7a resonance indicated that it must be the carbonyl substituted position allowing a 1(3*H*)-phthalide ring to be assigned. The moderately deshielded resonances of C-6 and C-7 indicated vicinal heteroatom substitution with the remaining amine and hydroxyl groups. The hydroxyl group was placed at the more deshielded C-6 position and the amine was located in the more shielded C-7 position. This heteroatom assignment was confirmed through the calculation of ^{13}C NMR data (Fig. 2). With the two-dimensional structure assigned, the absolute configuration of the C-3 stereogenic centre was assigned as a racemic mixture of the two enantiomers due to the lack of Cotton effects in the ECD spectrum and optical rotation. We propose that this is likely due to tautomerism under basic conditions that leads to the opening of the lactone and racemization of C-3. This also occurs in other phthalide based compounds including the dye phenolphthalein which undergoes the same tautomeric shift under basic pH conditions. This tautomerism and racemization have also been previously reported for a number of other compounds containing more similarly substituted phthalides.[11–13] The presence of a new UV maxima at ~360 nm

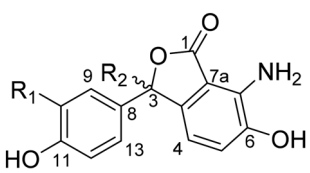

1: $R_1 = R_2 = H$
2: $R_1 = H$, $R_2 = COOCH_3$
3: $R_1 = I$, $R_2 = H$
4: $R_1 = I$, $R_2 = COOCH_3$

Fig. 1 Structures of the ascidiolides **1–4** isolated in this study.

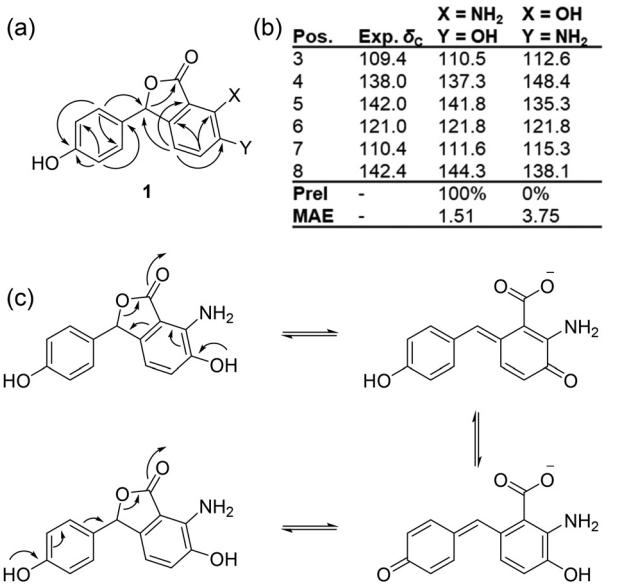

Pos.	Exp. δ_C	X = NH_2 Y = OH	X = OH Y = NH_2
3	109.4	110.5	112.6
4	138.0	137.3	148.4
5	142.0	141.8	135.3
6	121.0	121.8	121.8
7	110.4	111.6	115.3
8	142.4	144.3	138.1
Prel	-	100%	0%
MAE	-	1.51	3.75

Fig. 2 (a) Key HMBC correlations for the elucidation of **1**. (b) Comparison of calculated and experimental ^{13}C NMR shifts for two possible isomers of **1**. (c) Proposed tautomeric racemization of **1**.

under basic conditions is likely associated with the bathochromic shift of the keto form of the molecule.

Ascidiolide B (**2**) was isolated as a yellow amorphous solid and exhibited a protonated adduct $[M + H]^+$ at *m*/*z* 316.0816 in the (+)HRESIMS spectrum, consistent with the molecular formula $C_{16}H_{13}NO_6$. A comparison of the ^1H and ^{13}C NMR data between **1** and **2** indicated the absence of the C-3 proton signal and the presence of an additional carbonyl at δ_C 171.4 and an *O*-methyl at δ_H 3.76/δ_C 53.8 (s, OCH_3). HMBC correlations identified this as an *O*-methyl ester that was located at C-3. This assignment was also supported by the deshielded shift of H-4 (δ_H 6.76, d, J = 7.8 Hz) and H-9/13 (δ_H 7.19, d, J = 8.8 Hz, 2H). As with **1**, the molecule was identified as a racemic mixture due to the lack of Cotton effects in the ECD spectrum.

Ascidiolide C (**3**) was isolated as a yellow amorphous solid and was assigned the molecular formula $C_{14}H_{10}INO_4$ based on the protonated adduct $[M + H]^+$ detected by (+)HRESIMS at *m*/*z* 383.9727. The comparison of the ^1H NMR data between **1** and **3** indicated the presence of a 1,3,4-trisubstituted aromatic ring in place of the *para*-disubstituted one. The significant deshielding of H-9 (δ_H 7.56, d, J = 2.1 Hz) and shielding of C-10 (δ_C 84.0) along with the mass increase of 126.9 Da indicated unequivocally that the third substituent at C-10 was an iodine atom. Again compound **3** was assigned as a racemic mixture from the ECD.

Ascidiolide D (**4**) was isolated as a yellow amorphous solid and exhibited an intense molecular ion in the (+)HRESIMS data for $[M + H]^+$ at *m*/*z* 441.9782, consistent with the molecular formula $C_{16}H_{12}INO_6$. The ^1H and ^{13}C NMR data of **4** exhibited similarities with both compounds **2** and **3**. The presence of an *O*-methyl ester at δ_H 3.77 indicated the same core structure present in **2**. Furthermore, the loss of symmetry in the aromatic ring and additional non-protonated carbon at δ_C 85.0 indicated the presence of the same iodinated aromatic ring identified in **3**.

A LC-MS/MS profile of the initial extract indicated the presence of a number of other related metabolites (Fig. S6).[9] A combination of MS/MS and 2D NMR experiments was conducted on the fraction of *A. virginea* to investigate the structures of these minor derivatives. The MS^2 data of **1–4** were first analysed to identify common fragmentation patterns within the family (Fig. S5). This assignment then allowed the annotation of eight further derivatives **5–12** with different halogenation patterns (Fig. S7-1 to S7-12). The isotope pattern of the MS^1 and the fragmentation pattern in the MS^2 indicated the presence of different iodine or bromine substituents around the phenol ring. The MS^2 of **5–8** shared close similarities with **1** and **3**, allowing the protonated stereocentre to be assigned and **9–12** showed the typical fragment ions associated with the loss of the methyl ester and other related fragments. Particular signals present in the HSQC of the mixture allowed further confirmation of the halogenation positions with typical NMR shifts associated with either brominated or iodinated 4-hydroxyphenyl rings.[14]

A number of other peaks in the LC-MS chromatogram were also observed with similar fragmentation patterns. These had the same fragments associated with the methyl ester cleavage in compounds **2** and **4**, although they had differing precursor masses indicating the presence of a differing C-3 substituent. Five derivatives **13–17** were identified with a mass loss of *m*/*z* 32.0272 (Fig. S7-13 to S7-17), indicating the substitution of a methoxy group at C-3, and three derivatives **18–20** were identified with a C-3 hydroxyl substituent due to a loss of *m*/*z* 18.0104 (see the SI). The C-3 hydroxyl substituted ascidiolides **18–20** are similar to other γ-hydroxyfuranones commonly found in ascidians.[4,15,16] However, we suspect that the methoxy derivatives **13–17** are artefacts derived from **18–20** as products of the methanolysis of certain γ-hydroxyfuranones have previously been described.[17] To confirm this assumption, the LC-MS was rerun on a sample diluted in MeOH and left for 48 h. This led to a decrease in hydroxylated metabolites compared to the methoxylated derivatives, which is consistent with the assumed solvolysis (Fig. S12).

Most phthalide derivatives have been isolated from microbial and plant sources and typically originate from polyketides or terpenes. Ascidiolides A–D (**1–4**) represent the first phthalides isolated from tunicates and are unique due to the aniline substitution absent in polyketide or terpenoid derivatives. The ascidiolides are closely related to the previously reported iodinated isoquinolinediones, ascidines **21–23**, previously isolated from *A. virginea* collected in Norway (Fig. 3b).[10] However, while these two related families of natural products share the same halogenated hydroxyphenyl moiety, the core structures differ significantly. We assume that the ascidines and the new ascidiolides are likely derived from similar precursors, although the cyclization would differ leading to either an isoquinolinedione or a phthalide core, respectively. On review of the literature, only one family of metabolites, the dermacozines, was found to be related to both the ascidines and ascidiolide structures. The dermacozines are phenozine derivatives from deep sea actinomycetes.[18] Both the phthalide containing dermacozine D and the isoquinolinedione containing dermacozine E were isolated from the same culture. These were suggested to be formed from the condensation of dermacozine A with a hydroxyphenylglyoxylic acid precursor. Also of interest was the presence of dermacozine F containing a cyclic anhydride ring instead of the cyclic imide. Interestingly, unlike dermacozine D, E and F (Fig. S11), which were isolated together in our investigation of the Irish specimen of *A. virginea*, the ascidiolides were the only derivatives present and were not reported from the Norwegian specimen. The furanone moiety of the ascidiolides is also very similar to polyaromatic furanone derivatives, such as the rubrolides that are common among marine ascidians.[3–6] We assume that compounds **1–4** are related to other ascidian furanone derivatives through a similar biosynthetic condensation of two amino acid derived precursors. However, unlike ascidian furanone derivatives that are produced from the dimerization of two of the same precursors, the ascidiolides are likely derived from two completely different precursors. The hypothetical biosynthesis proposed for previous ascidian furanone derivatives[3,19] and the dermacozines[20] inspired our biosynthetic hypothesis for the new

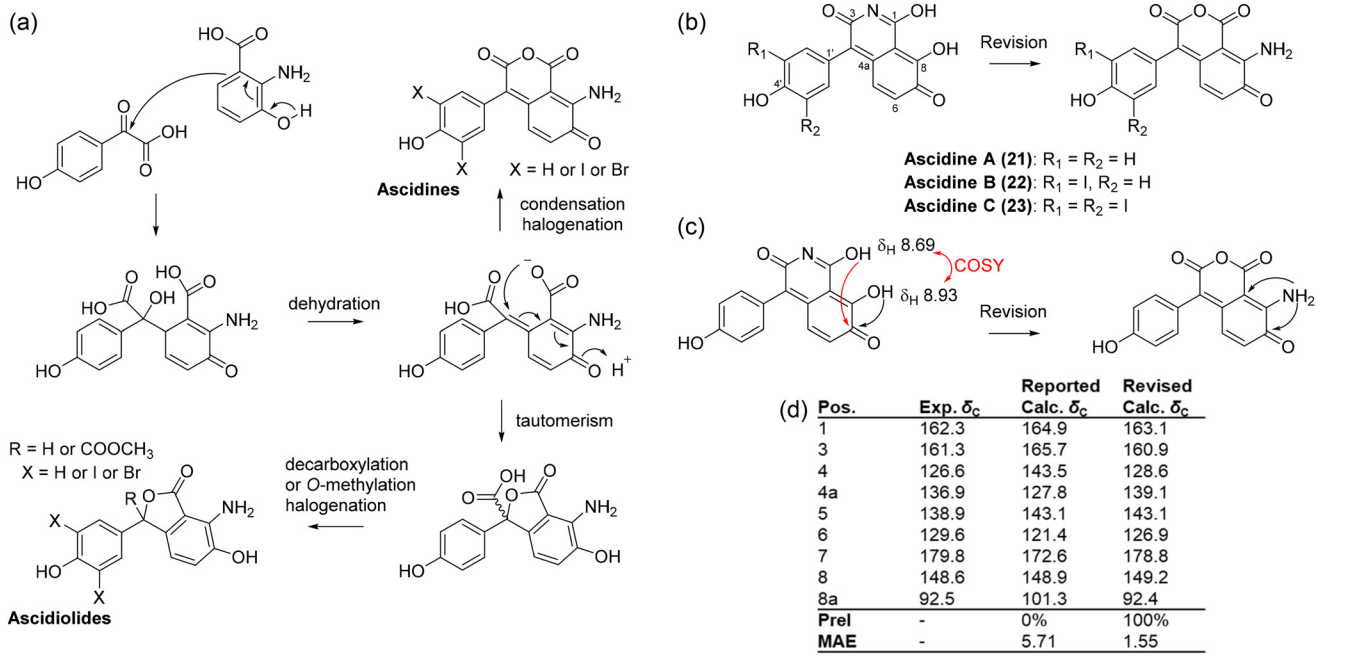

(d)

Pos.	Exp. δ_C	Reported Calc. δ_C	Revised Calc. δ_C
1	162.3	164.9	163.1
3	161.3	165.7	160.9
4	126.6	143.5	128.6
4a	136.9	127.8	139.1
5	138.9	143.1	143.1
6	129.6	121.4	126.9
7	179.8	172.6	178.8
8	148.6	148.9	149.2
8a	92.5	101.3	92.4
Prel	-	0%	100%
MAE	-	5.71	1.55

Fig. 3 (a) Proposed biosynthetic pathway of the ascidiolides and ascidines from 4-hydroxyphenylglyoxylic acid and 3-hydroxyanthranilic acid. (b) The proposed revision of the reported structures for the ascidines based on the proposed biosynthesis. (c) 2D NMR correlations of ascidine A (**21**) in red that do not support the published structure but instead support the proposed revision. (d) Comparison of the experimental ^{13}C NMR shifts with the calculated ^{13}C NMR shifts for the reported and revised structures. Relative probability (Prel) and mean absolute error (MAE) are presented for an overall statistical comparison.

ascidiolides and we suggest that these are produced from the cyclic condensation of 4-hydroxyphenylglyoxylic acid and 3-hydroxyanthranilic acid (Fig. 3a).

Unexpectedly, the position of the nitrogen in the ascidines suggests that their biosynthesis starts from an unusual 2,3-dihydroxybenzamide precursor, while the more common 3-hydroxyanthranilic acid is proposed to be the same precursor responsible for the production of the ascidiolides. 3-Hydroxyanthranilic acid is typically derived from tryptophan through the kynurenine biosynthetic pathway and it would be unlikely that 2,3-dihydroxybenzamide would be derived from the same pathway. Therefore, we reinvestigated the structures proposed for the ascidines using the supplementary data provided in their original report and additional calculations. On evaluation of the NMR data reported for the ascidines, some data did not correlate with the proposed structures. These include the unusual $^{5}J_{CH}$ HMBC correlation from the hydroxy proton at δ_H 8.69 (1-OH) to the quinone carbon (C-7) and the strong $^{6}J_{HH}$ COSY correlation between the two hydroxy protons at δ_H 8.69 (1-OH) and δ_H 8.93 (8-OH). Additionally, the hydroxy proton chemical shifts were not consistent with a shift expected for phenolic protons that would form hydrogen bonds (>10 ppm).[21–23] Furthermore, the cyclic imide type structure that is proposed based on IR bands would exist as a stable zwitterion with an NH proton instead of the phenolic proton proposed.[24] The only structure consistent with the NMR data would be with a cyclic anhydride, and the two protons at δ_H 8.69 and 8.93 are amine protons at the C-8 position (Fig. 3c). Not only would the proton chemical shifts be more appropriate for this group[25] but this would also explain the COSY and HMBC correlations observed. The calculation of NMR shifts with Gauge-Independent Atomic Orbital (GIAO) DFT has become a useful way to assign the correct structural isomers of natural products.[26] Therefore, to further confirm this revision, the ^{13}C NMR shifts of three different isomers for ascidine A (**21**) were calculated. The isotropic shielding tensors were calculated with a B3LYP-D3(BJ)/TZVP//ωB97X-D/6-31G* functional/basis set combination. A PCM model with DMSO was used for the NMR calculations. The shielding tensors were then converted to chemical shifts and compared to the published experimental data run in DMSO-d_6 using the Sorted Training Sets published for DMSO.[27] The calculated shifts for the revised structure exhibited a significantly closer match to the experimental shifts (Fig. 3d) and this revised structure had a relative probability of 100%. We suggest that the structures of the reported ascidines A–C (**21–23**) should be revised to 8-amino-isochromene-1,3,7-trione derivatives.

A number of phthalides from plants and microbes have been described with several bioactivities including central nervous system modulation, anti-cancer, anti-inflammation and antioxidant activity.[13,18,28] Furthermore, polyaromatic butenolides from ascidians have previously been shown to be weakly cytotoxic[6] and antibacterial,[4] as well as inhibit the aggregation of neurodegenerative disease associated proteins.[3,29] The related ascidian, *Ascidia nigra*, also produces the polyphenolic tunichromes that are important antioxidant

blood reducing agents.[30] We therefore conducted a broad screening on the isolated ascidiolides (**1–4**) for antimicrobial, antitumoral and antioxidant activity. Due to the initial brine shrimp toxicity of the fractionated extract, compounds **1–4** were first screened for their cytotoxic activity against a panel of tumour cell lines. None of the compounds exhibited a decrease of cell growth higher than 50% at concentrations up to 40 μg mL^{-1}. Ascidiolide D (**4**) exhibited the highest activity, decreasing cell viability of the A549 cell line by 31% at 40 μg mL^{-1}. The compounds were also tested for antimicrobial activity against a wide panel of pathogens. Only ascidiolide D (**4**) at the highest concentration (128 μg mL^{-1}) inhibited MRSA growth by 50%. The lack of activity from the isolated compounds compared with the initial extract could be due to a number of reasons. Further screening of the unpurified fraction exhibited greater activity against both tumour cells and microbial pathogens than **1–4**. This could indicate that some of the minor derivatives not isolated in this study (**5–20**) may have greater bioactivity or that a significant synergistic effect takes place between these compounds.

We also screened **1–4** for their antioxidative potential by evaluating their radical scavenging activity against stable DPPH. Ascidiolide D (**4**) showed the strongest radical scavenging activity with an IC_{50} of 9.5 μM, followed by **3** (IC_{50} 72 μM), **2** (IC_{50} 140 μM) and **1** (IC_{50} 220 μM). The activity of ascidiolide D (**4**) was comparable to that of ascorbic acid (IC_{50} 11 μM). These results indicate that both the iodine substituent and C-3 methyl ester separately led to greater radical scavenging activity. Given the tautomerism proposed within these phthalides, we evaluated the effect of iodine and C-3 methyl ester substitution on the pK_a of the phenol protons *in silico*. This indicated a significant decrease in the pK_a of the phenol protons with iodine substitution. It is assumed that the radical scavenging activity is highly dependent on this tautomeric pathway and therefore the diiodinated derivatives would potentially have even greater radical scavenging activity. This antioxidant activity may indicate that the ascidiolides may be important reducing agents within the organism similar to the tunichromes.

Conclusions

Ascidiolides are a new family of phthalides natural products isolated from the solitary ascidian *Ascidia virginea* from the North Atlantic. This study led to the isolation of four analogues and the proposal of a further 16 derivatives based on LC-MS/MS data. The structure of the ascidiolides led to the investigation and revision of the structure of the ascidines, the only other metabolites previously isolated from *A. virginea*. A notable geographic metabolite difference was observed for *A. virginea* with the ascidiolides identified from Irish waters and the ascidines from Norwegian waters. Ascidiolide D (**4**) exhibited the greatest activity with weak cytotoxicity and radical scavenging activity comparable to that of ascorbic acid.

Experimental

General experimental procedures

Optical rotations were recorded at the sodium D-line (589.3 nm) on a Rudolph Research Analytical Autopol IV polarimeter with a 5 × 100 mm cell at 20 °C (Rudolph Research Analytical, NJ, USA). UV and ECD were recorded in acetonitrile on a Chirascan V100 with a 1.0 cm quartz cuvette (Applied Photophysics, Leatherhead, UK). IR data were recorded on a PerkinElmer Spectrum 100 FT-IR spectrometer (Massachusetts, USA). NMR experiments were performed on a 600 MHz Agilent Premium Compact spectrometer with a 5 mm CryoProbe (Agilent, Santa Clara, USA). The chemical shifts (δ in ppm) are referenced to the carbon (δ_C 49.00 of CD_3OD) and proton (δ_H 3.31 of CHD_2OD) signals of residual non-deuterated solvent. Liquid chromatography high-resolution electrospray ionisation mass spectrometry (HRESIMS) and tandem mass spectrometry were performed on an Agilent 6540 Q-Tof mass spectrometer equipped with an Agilent 1290 UHPLC and auto-sampler (Agilent). RP-SPE fractionation was performed using Polygoprep C_{18}-bonded silica 50 μm, 100 Å (Labquip, Dublin, Ireland). Semipreparative HPLC was carried out on an Agilent 1260 HPLC system equipped with a DAD detector. Analytical HPLC was carried out on a Shimadzu HPLC system equipped with two LC-20AD pumps, an SIL-20AC auto-sampler, an SPD-M20A PDA detector and an FRC-10A fraction collector (Mason Tech., Dublin, Ireland). All solvents used for extraction and separation were of HPLC grade. Trifluoroacetic acid (TFA) used for HPLC separation was of spectroscopy grade from Alfa Aesar.

Biological materials

The marine ascidian, *Ascidia virginea*, was collected by scuba divers on the 16th of April 2018 from Croaghan Island, Co. Donegal, Ireland. This sample was identified based on morphology by Bernard Picton. A voucher specimen of this sample 'BDV10101' is stored at the Marine Biodiscovery Laboratory, School of Biological and Chemical Sciences, University of Galway (Co. Galway, Ireland).

Extraction and isolation

The freeze-dried ascidian material (3.8 g) was extracted with a 1 : 1 (v/v) mixture of MeOH/CH_2Cl_2 under sonication. The resulting extract (0.86 g) was then fractionated on C_{18} bonded silica, eluting with a stepwise gradient from H_2O to CH_2Cl_2. Fractions were eluted with 100% H_2O, 50% H_2O/50% MeOH (265.0 mg), 25% H_2O/75% MeOH (30.6 mg), 100% MeOH (49.6 mg), and 50% MeOH/50% CH_2Cl_2 (71.7 mg). The 25% H_2O/75% MeOH fraction was further separated using reversed-phase semipreparative HPLC purification on a Waters Symmetry C_{18} prep column (7 μm, 7.8 × 250 mm). The column was first eluted with 70% H_2O (0.1%TFA)/30% MeCN (0.1% TFA) for 5 min, followed by a linear gradient to 63% H_2O (0.1%TFA)/36% MeCN (0.1%TFA) over 18 min. Finally, a linear gradient to 100% MeCN (0.1%TFA) over 2 min was performed and the column was then further eluted under these con-

ditions for 10 min all at a flow rate of 2.2 mL min^{-1}. This yielded the new compounds ascidiolide A (**1**, 0.8 mg, 2.1 × 10^{-4}% dry wt), impure ascidiolide B (2.5 mg), ascidiolide C (**3**, 0.6 mg, 1.6 × 10^{-4}% dry wt), and impure ascidiolide D (2.6 mg). The impure ascidiolide D and B samples were further purified with the same reversed-phase analytical HPLC purification method on a Macherey-Nagel Nucleodur C_{18} column (5 μm, 4.6 × 250 mm). The column was first eluted with 90% H_2O (0.1%TFA)/10% MeCN (0.1%TFA) for 5 min, followed by a linear gradient to 40% H_2O (0.1%TFA)/60% MeCN (0.1%TFA) over 20 min. Finally, a linear gradient to 100% MeCN (0.1% TFA) over 5 min was performed and the column was further eluted with 100% MeCN (0.1%TFA) for 7 min, all at a flow rate of 1.0 mL min^{-1}. This yielded pure ascidiolide B (**2**, 1.0 mg, 2.6 × 10^{-4}% dry wt) and ascidiolide D (**4**, 1.3 mg, 3.4 × 10^{-4}% dry wt).

Ascidiolide A (1). Light red amorphous solid; $[\alpha]_{20}^{D}$ 0 (*c* 0.02, MeOH); UV/Vis (*c* 0.25 mM, H_2O) λ_{max} (log ε) 190 (3.63) nm; ^{1}H NMR and ^{13}C NMR data (see Table 1); (+)HRESIMS *m*/*z* 258.0765 $[M + H]^+$ (calcd for $C_{14}H_{29}N_4O_2^+$, 258.0761, Δ −1.5 ppm).

Ascidiolide B (2). Yellow amorphous solid; $[\alpha]_{20}^{D}$ 0 (*c* 0.08, MeOH); UV/Vis (*c* 0.14 mM, H_2O) λ_{max} (log ε) 192 (4.24) nm; ^{1}H NMR and ^{13}C NMR data (see Table 1); (+)HRESIMS *m*/*z* 316.0818 $[M + H]^+$ (calcd for $C_{14}H_{29}N_4O_2^+$, 316.0816, Δ +0.6 ppm).

Ascidiolide C (3). Yellow amorphous solid; $[\alpha]_{20}^{D}$ 0 (*c* 0.08, MeOH); UV/Vis (*c* 0.13 mM, H_2O) λ_{max} (log ε) 190 (4.28) nm; ^{1}H NMR and ^{13}C NMR data (see Table 1); (+)HRESIMS *m*/*z* 383.9726 $[M + H]^+$ (calcd for $C_{14}H_{29}N_4O_2^+$, 383.9727, Δ −0.3 ppm).

Ascidiolide D (4). Reddish yellow amorphous solid; $[\alpha]_{20}^{D}$ 0 (*c* 0.08, MeOH); UV/Vis (*c* 0.19 M, H_2O) λ_{max} (log ε) 190 (4.14) nm; IR (film) ν_{max} 3331, 2952, 1690, 1154, 1111, 980 cm^{-1}; ^{1}H NMR and ^{13}C NMR data (see Table 1); (+)HRESIMS *m*/*z* 441.9783 $[M + H]^+$ (calcd for $C_{14}H_{29}N_4O_2^+$, 441.9782, Δ +0.2 ppm).

Further LC-MS analysis was performed on an Agilent QTOF 6540 equipped with a Dual Agilent Jet Stream (Dual-AJS) electrospray ionization source. The mass spectrometer was coupled to an Agilent UPLC 1290 Infinity. Chromatographic separation was performed on a Waters Acquity UHPLC BEH C_{18} column (1.7 μm, 2.1 mm × 100 mm). Multiple different LC methods were tested and the selected one eluted samples with 90% H_2O (0.1% FA)/10% MeCN (0.1% FA) at 0.5 mL min^{-1} for 2 min, followed by a linear gradient to 50% MeCN (0.1% FA) over 6 min, and further elution at this percentage for 4 min. Mass spectra were acquired in +ESI mode with parameters set to a VCap of 3.5 kV, a nozzle voltage of 1.0 kV, a gas temperature of 300 °C at a flow of 11 L min^{-1}, a sheath gas temperature of 325 °C at a flow of 8 L min^{-1}, and a nebulizer pressure at 35 psig. The mass range was fixed at 100–1700 Da for the MS^1 and MS^2 acquisition. The acquisition rates were set at 3 spectra per s for both MS^1 and MS^2. The collision energy was fixed at 35 V. Both untargeted and targeted MS/MS were used to obtain clear MS^2 of potential derivatives. In untargeted runs, the same mass was excluded for 0.3 min after 4 spectra were acquired and no exclusion was set for targeted runs. Data were analysed and spectra were produced using MassHunter Qualitative software (Agilent).

Computational methods

A conformational analysis of two isomers of ascidiolide A (**1**) and three isomers of ascidine A (**21**) was performed with Schrodinger MacroModel. This conformer generation was performed using the OPLS3 force field with an energy window of 5.0 kcal mol^{-1}. The conformers generated were further optimized using DFT, at the B3LYP-D3(BJ)/TZVP level in Gaussian 16, and at the same time, the free energy of each conformer was calculated.[31] The isotropic shielding tensors for each conformer were then calculated by using GIAO in Gaussian 16 at the ωB97X-D/6-31G* level. A polarizable continuum solvation

Table 1 NMR spectroscopic data for ascidiolides A–D (**1–4**) in CD_3OD

	Ascidiolide A (**1**)		Ascidiolide B (**2**)		Ascidiolide C (**3**)		Ascidiolide D (**4**)	
Pos.	δ_C, type	δ_H (*J* in Hz)	δ_C, type	δ_H (*J* in Hz)	δ_C, type	δ_H (*J* in Hz)	δ_C, type	δ_H (*J* in Hz)
1	174.2, C		172.0, C		173.3[a], C		171.8, C	
3	84.4, CH	6.25, br s	89.5, C		83.1, CH	6.22, br s	88.4, C	
3a	142.4, C		138.7, C		141.9, C		138.7, C	
4	110.4, CH	6.30, dd (7.6, 0.9)	112.4, CH	6.76, d (7.8)	110.1, CH	6.32, dd (7.8, 0.9)	112.2, CH	6.75, d (7.8)
5	121.0, CH	6.92, d (7.6)	120.3, CH	6.99, d (7.8)	121.0, CH	6.93, d (7.8)	120.4, CH	7.01, d (7.8)
6	145.0, C		146.2, C		145.2, C		146.5, C	
7	138.0, C		138.4, C		137.7[a], C		137.8, C	
7a	109.4, C		108.5, C		108.7[a], C		108.2, C	
8	129.9, C		129.2, C		132.0, C		129.3, C	
9	130.0, CH	7.07, d (8.5)	129.3, CH	7.19, d (8.8)	139.5, CH	7.56, d (2.1)	138.9, CH	7.64, d (2.2)
10	116.5, CH	6.77, d (8.5)	116.3, CH	6.76, d (8.8)	84.0[a], C		85.0, C	
11	159.4, C		159.5, C		158.5[a], C		159.8, C	
12	116.5, CH	6.77, d (8.5)	116.3, CH	6.76, d (8.8)	115.8, CH	6.81, d (8.3)	115.7, CH	6.79, d (8.5)
13	130.0, CH	7.07, d (8.5)	129.3, CH	7.19, d (8.8)	129.8, CH	7.07, dd (8.3, 2.1)	129.3, CH	7.22, dd (8.4, 2.2)
CO			171.4, C				171.0, C	
OCH_3			53.8, CH_3	3.76, s			53.9, CH_3	3.77, s

^{1}H NMR was measured at 600 MHz and ^{13}C NMR was measured at 150 MHz. [a] δ_C resonance taken from HMBC data.

model was used with DMSO as a solvent for the NMR calculations.[32] The shielding tensors were then extracted, converted to chemical shifts and compared with the experimental shifts using the reported Sorted Training Sets method in DMSO.[27]

Biological assays

Antimicrobial growth inhibition assays were conducted against methicillin-resistant *S. aureus* (MB53963), *E. coli* (ATCC25922), *C. albicans* (ATCC64124), *A. baumannii* (MB5973), *P. aeruginosa* (PAO-1) and *A. fumigatus* (ATCC46645) following previously published procedures.[33] Compounds were assayed with 2-fold dose response curves starting at 128 μg mL^{-1}.

Cell viability assay using MTT (3-(4,5-dimethylthiazol-2-yl)-2,5-diphenyltetrazolium bromide) was conducted against five different human cancer cell lines A549 (lung carcinoma, CRM-CCL-185TM, ATCC), A2058 (metastatic melanoma, CRL-3601TM, ATCC), MCF7 (breast adenocarcinoma, HTB-22, ATCC), MIA PaCa-2 (pancreatic carcinoma, CRL-1420, ATCC), and Hep G2 (hepatocyte carcinoma, HB-8065, ATCC).[34] Compounds were assayed with 2-fold dose response curves starting at 40 μg mL^{-1}.

A quantitative spectrophotometric radical scavenging assay using stable DPPH (2,2-diphenyl-2-picrylhydrazyl hydrate, Alfa Aesar) was carried out in 96-well plates.[35] The ascidiolides (**1–4**) were prepared at a range of concentrations (1–256 μM) in 100 μL of MeOH. These samples were then added to 100 μL of a 100 μM solution of DPPH in MeOH and mixed in a micro-well. The plate was placed at room temperature for 30 min in the dark before measuring the absorption at 495 nm on a UV-Vis 96-well microplate spectrometer (BioTek EL808, Mason Technology, Ireland). All experiments were performed in triplicate, using ascorbic acid as a positive control. The percentage reduction was calculated using the absorption of a stable DPPH blank and a test compound blank.

Conflicts of interest

There are no conflicts to declare.

Data availability

The data supporting this article have been included as part of the SI: NMR and MS/MS spectra. See DOI: **https://doi.org/10.1039/d5ob01206f**.

The raw data can be made available upon request.

Acknowledgements

This project (Grant-Aid Agreements No. PDOC/19/02/01) was carried out with the support of the Marine Institute and funded under the Marine Research Programme by the Irish Government. We would like to acknowledge Bernard Picton and Christine Morrow for their expertise in the collection and identification of the ascidian. We would like to acknowledge the Irish Centre for High-End Computing (ICHEC) for access to computational resources and support. Part of this work has also been funded through the Interreg projects BEAP-MAR and Marinnonet (Atlantic Area, EAPA_0032/2022 and EAPA_0017/2022) and the Horizon Europe project COMBO (HORIZON-CL6-2023-CIRCBIO-01-11, 101135438).

References

1 A. R. Carroll, B. R. Copp, R. A. Davis, R. A. Keyzers and M. R. Prinsep, *Nat. Prod. Rep.*, 2021, **38**, 362–413.
2 G. Santaniello, A. Nebbioso, L. Altucci and M. Conte, *Mar. Drugs*, 2023, **21**, 24.
3 L. K. Jennings, L. P. Robertson, K. E. Rudolph, A. L. Munn and A. R. Carroll, *J. Nat. Prod.*, 2019, **82**, 2620–2626.
4 J. Bracegirdle, L. J. Stevenson, A. V. Sharrock, M. J. Page, J. A. Vorster, J. G. Owen, D. F. Ackerley and R. A. Keyzers, *J. Nat. Prod.*, 2021, **84**, 544–547.
5 C. J. Smith, R. L. Hettich, J. Jompa, A. Tahir, M. V. Buchanan and C. M. Ireland, *J. Org. Chem.*, 1998, **63**, 4147–4150.
6 A. R. Carroll, P. C. Healy, R. J. Quinn and C. J. Tranter, *J. Org. Chem.*, 1999, **64**, 2680–2682.
7 S. K. Palanisamy, O. P. Thomas and G. P. McCormack, *Bioengineered*, 2018, **9**, 55–60.
8 M. M. Reddy, L. Jennings and O. P. Thomas, in *Progress in the Chemistry of Organic Natural Products*, ed. A. D. Kinghorn, H. Falk, S. Gibbons, Y. Asakawa, J. K. Liu and V. M. Dirsch, Springer, Cham, 2021, vol. 116, pp. 1–36.
9 S. Afoullouss, A. Balsam, A. L. Allcock and O. P. Thomas, *Mar. Drugs*, 2022, **12**, 245.
10 S. T. Possner, F. C. Schroeder, H. T. Rapp, V. Sinnwell, S. Franke and W. Francke, *Z. Naturforsch., C: Biosci.*, 2017, **72**, 259–264.
11 G. Strobel, E. Ford, J. Worapong, J. K. Harper, A. M. Arif, D. M. Grant, P. C. W. Fung and R. M. W. Chau, *Phytochemistry*, 2002, **60**, 179–183.
12 J. K. Harper, A. M. Arif, E. J. Ford, G. A. Strobel, J. A. Porco, D. P. Tomer, K. L. Oneill, E. M. Heider and D. M. Grant, *Tetrahedron*, 2003, **59**, 2471–2476.
13 L.-H. Meng, A. Mándi, X.-M. Li, Y. Liu, T. Kurtán and B.-G. Wang, *Chirality*, 2016, **28**, 581–584.
14 P. O. Guillen, K. B. Jaramillo, L. Jennings, G. Genta-Jouve, M. de la Cruz, B. Cautain, F. Reyes, J. Rodríguez and O. P. Thomas, *J. Nat. Prod.*, 2019, **82**, 1354–1360.
15 D. W. Prebble, D. C. Holland, J. B. Hayton, F. Ferretti, L. K. Jennings, J. Everson, M. Xu, M. J. Kiefel, G. D. Mellick and A. R. Carroll, *J. Nat. Prod.*, 2023, **86**, 533–540.
16 S. Miao and R. J. Andersen, *J. Org. Chem.*, 1991, **56**, 6275–6280.
17 R. J. Capon, *Nat. Prod. Rep.*, 2020, **37**, 55–79.
18 W. M. Abdel-Mageed, B. F. Milne, M. Wagner, M. Schumacher, P. Sandor, W. Pathom-aree, M. Goodfellow, A. T. Bull, K. Horikoshi, R. Ebel, M. Diederich, H.-P. Fiedler and M. Jaspars, *Org. Biomol. Chem.*, 2010, **8**, 2352–2362.

19 J. Bracegirdle, L. J. Stevenson, M. J. Page, J. G. Owen and R. A. Keyzers, *Mar. Drugs*, 2020, **18**, 337.
20 W. M. Abdel-Mageed, B. Juhasz, B. Lehri, A. S. Alqahtani, I. Nouioui, D. Pech-Puch, J. N. Tabudravu, M. Goodfellow, J. Rodríguez, M. Jaspars and A. V. Karlyshev, *Mar. Drugs*, 2020, **18**, 131.
21 Y. Ohkawa, K. Miki, T. Suzuki, K. Nishio, T. Sugita, K. Kinoshita, K. Takahashi and K. Koyama, *J. Nat. Prod.*, 2010, **73**, 579–582.
22 Z.-K. Guo, Y.-Q. Zhou, H. Han, W. Wang, L. Xiang, X.-Z. Deng, H.-M. Ge and R.-H. Jiao, *Mar. Drugs*, 2018, **16**, 45.
23 H. Liu, Z. Chen, G. Zhu, L. Wang, Y. Du, Y. Wang and W. Zhu, *Tetrahedron*, 2017, **73**, 5451–5455.
24 P. T. McKittrick and J. E. Katon, *Appl. Spectrosc.*, 1990, **44**, 812–817.
25 G. Carr, W. Tay, H. Bottriell, S. K. Andersen, A. G. Mauk and R. J. Andersen, *Org. Lett.*, 2009, **11**, 2996–2999.
26 M. O. Marcarino, S. Cicetti, M. M. Zanardi and A. M. Sarotti, *Nat. Prod. Rep.*, 2022, **39**, 58–76.
27 J. Li, J.-K. Liu and W.-X. Wang, *J. Org. Chem.*, 2020, **85**, 11350–11358.
28 Y. Chen, Q. Cheng, S. Lv, Z. Kang and S. Zeng, *Heliyon*, 2023, **9**, e22957.
29 D. C. Holland, D. W. Prebble, S. Er, J. B. Hayton, L. P. Robertson, V. M. Avery, A. Domanskyi, M. J. Kiefel, J. N. A. Hooper and A. R. Carroll, *J. Nat. Prod.*, 2022, **85**, 441–452.
30 E. M. Oltz, R. C. Bruening, M. J. Smith, K. Kustin and K. Nakanishi, *J. Am. Chem. Soc.*, 1988, **110**, 6162–6172.
31 M. J. Frisch, G. W. Trucks, H. B. Schlegel, G. E. Scuseria, M. A. Robb, J. R. Cheeseman, G. Scalmani, V. Barone, G. A. Petersson, H. Nakatsuji, X. Li, M. Caricato, A. V. Marenich, J. Bloino, B. G. Janesko, R. Gomperts, B. Mennucci, H. P. Hratchian, J. V. Ortiz, A. F. Izmaylov, J. L. Sonnenberg, D. Williams-Young, F. Ding, F. Lipparini, F. Egidi, J. Goings, B. Peng, A. Petrone, T. Henderson, D. Ranasinghe, V. G. Zakrzewski, J. Gao, N. Rega, G. Zheng, W. Liang, M. Hada, M. Ehara, K. Toyota, R. Fukuda, J. Hasegawa, M. Ishida, T. Nakajima, Y. Honda, O. Kitao, H. Nakai, T. Vreven, K. Throssell, J. A. Montgomery Jr, J. E. Peralta, F. Ogliaro, M. J. Bearpark, J. J. Heyd, E. N. Brothers, K. N. Kudin, V. N. Staroverov, T. A. Keith, R. Kobayashi, J. Normand, K. Raghavachari, A. P. Rendell, J. C. Burant, S. S. Iyengar, J. Tomasi, M. Cossi, J. M. Millam, M. Klene, C. Adamo, R. Cammi, J. W. Ochterski, R. L. Martin, K. Morokuma, O. Farkas, J. B. Foresman and D. J. Fox, *Gaussian 16 Rev. C.01*, Wallingford, CT, 2016.
32 J. Tomasi, B. Mennucci and R. Cammi, *Chem. Rev.*, 2005, **105**, 2999–3094.
33 M. C. Monteiro, M. de la Cruz, J. Cantizani, C. Moreno, J. R. Tormo, E. Mellado, J. R. De Lucas, F. Asensio, V. Valiante, A. A. Brakhage, J.-P. Latgé, O. Genilloud and F. Vicente, *J. Biomol. Screening*, 2012, **17**, 542–549.
34 K. Präbst, H. Engelhardt, S. Ringgeler and H. Hübner, in *Cell Viability Assays: Methods and Protocols*, ed. D. F. Gilbert and O. Friedrich, Springer New York, New York, NY, 2017, pp. 1–17.
35 L. R. Fukumoto and G. Mazza, *J. Agric. Food Chem.*, 2000, **48**, 3597–3604.